Appendix E2. Hayward and Chabot Fault Location Uncertainty Evaluation for a Utility Corridor

Lettis Consultants International, Inc.
1000 Burnett Avenue, Suite 350
Concord, CA 94520
(925) 482-0360; fax (925) 482-0361

EARTH SCIENCE CONSULTANTS

Date: January 30, 2024

To: Chris Madugo
Geosciences Department
Pacific Gas & Electric Company
C7M0@pge.com

SUBJECT: **Hayward and Chabot Fault Location Uncertainty Evaluation for a Utility Corridor – Oakland, CA**

Dear Dr. Madugo,

Lettis Consultants International, Inc. (LCI) is pleased to submit this fault location evaluation along Pacific Gas and Electric Company (PG&E)'s Moraga-Oakland utility corridor in Oakland, California. This desktop and field reconnaissance study focused on evaluating the uncertainty in fault location for strands of the Hayward and Chabot faults within the utility corridor northeast of Highway 13, which was defined by PG&E at the start of the project (Figure 1). Other consultants (InfraTerra, 2021) evaluated the utility corridor on the southwest side of Highway 13.

Executive Summary

To assist with locating PG&E infrastructure, this evaluation provides information characterizing the location of the Hayward and Chabot faults in the vicinity of the Moraga-Oakland utility corridor (Figure 1). LCI's evaluation includes documentation of fault information and location uncertainty based on review of publications, geologic mapping, and available published fault studies. LCI agrees with past work by the California Geologic Survey (CGS) and other studies that conclude (1) the Hayward fault a Holocene active fault and (2) the Chabot fault is not a Holocene active fault. LCI assumes that fault rupture can occur anywhere within either fault location uncertainty zone shown in Figure 2.

1.0 SCOPE OF WORK

The scope of work for this evaluation included data compilation/review/analysis (Task 1), geomorphic analysis and field reconnaissance (Task 2), defining uncertainty zones (Task 3), and reporting (Task 4). As part of Task 1, LCI reviewed available geologic maps, lidar data, historical aerial photos, and available fault studies including trench studies from Alquist Priolo investigations and fault evaluation reports. LCI also reviewed mapping and creep data along the mapped Hayward fault and evaluated geomorphic or structural evidence to constrain the location of the Chabot fault. LCI (Ian McGregor and Robert Givler) and PG&E (Christopher Madugo) personnel completed field reconnaissance in the site vicinity on Wednesday January 17th. LCI's field waypoints (or localities) are shown on Figures 1 and 2. LCI used empirically derived datasets with additional criteria from field data to define and modify fault location uncertainty zones (Task 3). The results of this data compilation and analyses are shown in Field Photos1 through 3 and Figures 1 and 2.

2.0 HAYWARD FAULT

This section provides a summary of the tectonic setting of this part of the San Francisco Bay area, a discussion of the Hayward and Chabot faults, and information used to delineate surface fault traces at the Moraga-Oakland utility corridor (Figure 1).

2.1 TECTONIC SETTING: SAN FRANCISCO BAY AREA

The Moraga-Oakland utility corridor on the northeast side of Highway 13 in Oakland, CA is within the seismically active San Francisco Bay Region (SFBR) (Schwartz et al., 2014; WGCEP, 2003 and 2008). On a regional scale, the SFBR formed from distributed deformation and right-lateral shear associated with the development of the San Andreas Fault System, which accommodates approximately 36 to 43 mm/yr (1.4 to 1.7 in/yr) of distributed, northwest-directed motion between the Pacific plate and Sierran microplate (WGCEP, 2003; d'Alessio et al., 2005; Evans et al. 2012; Schwartz et al., 2014). The Sierran microplate lies between the Pacific and North America plates. Relative plate motion is primarily distributed across a series of north-northwest-striking, right-lateral strike-slip faults that include the San Andreas, Hayward, Rodgers Creek, Calaveras, and Greenville faults (Schwartz et al., 2014; WGCEP, 2003; 2008; Field et al., 2013; Johnson et al., 2022).

The Hayward fault represents the central part of a 195-mi-long (314-km-long) Rodgers Creek-Hayward- Calaveras fault system (Figure 1). The most recent Uniform California Earthquake Rupture Forecast (UCERF 3.0) (Field et al., 2015) assigns a probability of 32% that the Hayward-Rodgers Creek fault (HRCF) will produce an earthquake of M≥6.7 in the next 30 years, the highest probability for any SFBR fault other than the San Andreas fault (Figure 1). The 80-mi-long (130 km) Hayward fault is mapped along the western margin of the Diablo Range through the many urbanized communities of the SFBR (WGCEP 2003; Lienkaemper et al., 2014).

The Hayward fault is a northwest-striking, dextral fault characterized by 1) moderate aseismic creep rates (~4.0-7.2 mm/yr) (Lienkaemper et al., 2014; McFarland et al., 2017), 2) an alignment of microseismicity and historical earthquakes (e.g., 1868 M6.5±0.2 earthquake), and a 3) relatively simple fault geometry (in some cases it includes two creeping traces) with local structural complexities (Lienkaemper, 1992; 2006; Lettis, 2001) (Figure 1). Detailed studies of aseismic creep-related deformation and a compilation of fault studies by Lienkaemper et al. (1992; 2006) help to constrain fault location along much of the fault length. The long-term geologic slip rate is estimated at multiple locations along the fault (Williams, 2011; Lienkaemper and Borchardt, 1996). Dawson and Weldon (2013) use these data to estimate the long-term geological rate for the northern and southern sections of the Hayward fault at 10.4±2.0 and 9.2 ±1.4 mm/yr, respectively, for the Uniform California Earthquake Rupture Forecast, version 3 (UCERF3) (Field et al., 2013).

The Chabot fault is a northwest-striking, steeply east-dipping fault that is considered a splay of the larger, more-active Hayward fault system (Ponce, 2003; Graymer, 2006). Mapping and characterization of the Chabot in the vicinity of the utility corridor is based on the contact between Jurassic-aged serpentinite, volcanic, and mélange units on the southwest and Cretaceous marine sedimentary units of the Great Valley sequence on the northeast (Case, 1968; Radbruch, 1969; Graymer, 2000). The Chabot fault is considered to have long-term normal offset inferred from the structural and stratigraphic relief across the structure (Graymer, 2000) (Figure 1).

In the vicinity of the utility corridor, the Hayward fault is zoned within an Alquist-Priolo fault zone (A-P zone) as a Holocene active fault by the California Geological Survey (Radbruch and Hall, 1974; Herd, 1978). The Chabot fault was determined not to have sufficient evidence for Holocene activity and therefore was not considered in the revised A-P zone (Herd, 1978).

2.2 Site Geology at the Moraga-Oakland Utility Corridor

At the site, several traces of the Hayward and the Chabot faults are mapped intersecting the Moraga-Oakland utility corridor (Figure 1). In the southwestern portion of the study area, an eastern and western trace of the Hayward fault are mapped by PG&E (2022), Lienkaemper (2008), and Graymer (2000).

The western trace of the Hayward fault is mapped by Lienkaemper (2008) as a series of discontinuous northwest striking, right-stepping, en-echelon traces ranging from 800 to 1,500 ft in length (Figure 1). These traces are entirely within Jurassic graywacke/ meta graywacke basement rocks, but cut through Pleistocene gravels (Graymer, 2000). In the vicinity of the Moraga-Oakland utility corridor, Lienkaemper (2008) constrains the western trace through several field observations of creep (i.e., en-echelon cracks, offset curbs and fences) along the fault and alignment arrays that identify specific fault locations. Lienkaemper (2008) interprets the eastern Hayward fault strand as containing an extensional component, which is consistent with the en echelon pattern of faulting, arcuate shapes of surface traces, and Quaternary depocenters along the fault currently occupied by Highway 13. Radbruch and Hall (1974) and Herd (1978) generally delineated the eastern trace of the fault as a series of west-facing scarps in Pleistocene alluvium, linear drainages, and deflected drainages. Fault Evaluation Report No. 102 (Smith, 1980) modified mapping by Radbruch (1969) to conform to additional tectonic geomorphic features mapped along its trace. PG&E (2022) adopts the mapping by Lienkaemper (2008) in the V15 database.

The eastern trace of the Hayward fault (PG&E, 2022 V15 fault database) was originally mapped by Radbruch (1969) as an alignment of saddles and scarps in Pleistocene alluvium and was included by Herd (1978). The PG&E V15 (2022) eastern Hayward fault trace is generally coincident with a faulted contact between graywacke/ meta-graywacke and Franciscan complex mélange as mapped by Graymer (2000), but more closely follows the topographic break in slope within Pleistocene alluvium through the corridor. The discontinuous eastern trace makes a small, 22 m (72 ft) left step across Shepherd and Palo Seco Creek before crossing the western trace of the Hayward fault approximately 1,300 ft northwest of the utility corridor. This trace is interpreted to continue along strike of the lithologic contact mapped by Graymer (2000).

The published geologic map of Graymer (2000) shows the Chabot fault as the contact between Jurassic volcanics/ mélange (Jsv and Jb)/ Serpentinite (sp) and Late Cretaceous sedimentary rocks of the Joaquin Miller Formation and Oakland conglomerate (Kjm/ Ko). Other faulted contacts are interpreted within the Jurassic section (e.g., a subparallel strand juxtaposing Jsv and fs), however the most notable structural relief occurs along the Chabot fault. The Chabot fault is identified in the topography as the northeastern margin of a linear strike ridge formed by weather resistant, Jurassic basalt (Jb) and Serpentinite (sp) and aligned geomorphic features (see further descriptions below). Herd (1978) maps the fault as a series of truncated spurs and scarps, and notes that Radbruch (1969) depicts the fault as buried by Quaternary alluvium. The Chabot fault is not included in Alquist Priolo re-zoning and is classified as a Pleistocene or older structure that is not Holocene active. This assessment is consistent with findings from ESA/ WLA (1996) that found evidence to argue for the absence of fault activity in the last 35,000 years.

2.2.1 Alquist-Priolo (AP) Fault Studies in the Site Vicinity

In the site vicinity, LCI reviewed available A-P fault studies, including (Western Geologic Consultants, 1976; Peter Kaldveer and Associates, Inc. 1985; 1988; Purcell, Rhoades and Associates Inc., 1985; and JCP, 1980). These studies are briefly summarized below.

Western Geological Consultants (WGC, 1976) conducted a fault investigation for a site within the utility corridor approximately 150 ft northeast of the PG&E V15 eastern Hayward fault trace (Figures 1 and 2). The investigation included site reconnaissance and review of geologic maps and aerial imagery. This study did not identify faulting within the study area but observed potential slippage and settlement on the slope south of Scout Road. They contributed this observation to shallow settlement of soils around an existing sewer line.

Peter Kaldveer and Associates Inc. (1988) conducted a fault investigation for a site approximately 400 ft northwest of the Moraga-Oakland utility corridor area of interest and between the eastern Hayward and Chabot faults (Figures 1 and 2). The investigation included review of geologic maps and aerial imagery, drilling of exploratory probes, and fault trenching within the special studies zone. This study did not identify evidence of faulting within the two fault trenches or exploratory drilling.

Peter Kaldveer and Associates Inc. (1985) conducted a fault investigation for a site approximately 1,125 ft northwest of the Moraga-Oakland utility corridor area of interest and just northeast of the Hayward fault strand where PG&E V15 fault database depicts the western and eastern traces as intersecting (Figures 1 and 2). The investigation included review of geologic maps and aerial imagery, drilling/ logging exploratory bores, and exploratory trenching. This study did not identify evidence of faulting within fault trenches or exploratory drilling.

Further northwest, Purcell, Rhoades and Associates Inc. (1985) conducted a fault investigation for a site within 50 ft of the western Hayward fault trace (Figures 1 and 2). The investigation consisted of review of geologic maps and aerial imagery, site reconnaissance, and fault trenching within the special studies zone. This study did not identify evidence of faulting within the desktop analysis or trenching.

JCP (1980) conducted a fault investigation for a site area that included a concealed fault contact mapped by Graymer (2000), which was less than 100 ft west of the Chabot fault (Figures 1 and 2). The investigation included review of geologic maps and aerial imagery, detailed site reconnaissance, and fault trenching within the special studies zone. This study concluded that the fault mapped through the site is not active and did not identify other evidence of surface faulting.

2.2.2 Geomorphic Evaluation of the Hayward and Chabot Faults in the Site Area

This assessment evaluated the potential fault-related geomorphology along mapped faults in the vicinity of the Moraga-Oakland utility corridor (site area), east of Highway 13 (Figure 1). This evaluation was completed using a combination of lidar (USGS, 2021) and historical aerial photography from 1939 (Flight C-5750, Frames 289-44 and 289-45). The 1939 aerial photographs were effective in the geomorphic analysis because these photos pre-date most development in the area.

Interpretation of the 1939 aerial photography show the Chabot fault trace is delineated by an alignment of geomorphic features within the Moraga-Oakland utility corridor area of interest, including deflected drainages, aligned saddles and linear drainages. For example, in the northwestern portion of the study area (Figure 1), an approximately 1,200 ft long, northwest-striking southwest-facing topographic break in slope on the southwest margin of the Piedmont Hills is aligned with the right-deflection point of the Shepherd Creek. Southeast of Shepherd Creek, a linear trough/ shoulder and linear drainage channel further southwest are all aligned along a northwest orientation, which are subparallel to the mapped Chabot fault from Graymer (2000). Further southeast, linear drainages and ridges are consistently aligned along this orientation. Lastly, the linear drainages and troughs that bound the northeast margin of the linear ridge formed along the fault lineament are a persistent feature in the topography to the southeast outside of the study area.

The Hayward fault is geomorphically well-expressed in the 1939 aerial photograph (considerably more than the Chabot fault). Fault-related geomorphic features along the eastern and western traces of the Hayward fault proximal to the Moraga-Oakland utility corridor consist of a tight alignment of southwest-facing scarps in alluvium, linear troughs, slope breaks, and linear/ deflected drainages (Figure 1). In the western part of the Moraga-Oakland utility corridor area of interest, the eastern Hayward fault trace is mapped as an alignment of southwest-facing scarps, slope breaks (field localities 2 and 4; Figure 1), and linear troughs.

2.2.3 Moraga-Oakland Utility Corridor Field Reconnaissance

LCI's field reconnaissance focused on targeted observation of available rock outcrops/ preserved topographic features for field verification of geologic contacts mapped by Graymer (2000) that are pertinent to identifying the location and width of the Hayward and Chabot faults (Figure 1). Additionally, geomorphic lineaments mapped during this study were investigated in the field to assist in locating evidence of surface deformation.

Overall, this field reconnaissance allowed LCI to confirm and refine the location of the Hayward and Chabot fault in the vicinity of the Moraga-Oakland utility corridor to help develop the fault location uncertainty zones. Important field localities are summarized below.

At Field Locality 3, LCI mapped the location of the Chabot fault (Figures 1 and 2) on Shepard Canyon Road near the Oakland Fire Station No. 24, where a roadcut exposure of dark gray basalt/ mélange rocks (Jsv/ Jb units) on the west were observed juxtaposed against thinly to moderately bedded brown shale (Kjm unit) on the east side. This contact zone was semi-obscured by slope wash material; however, the contact occurred as a narrow zone (3 to 6 m or roughly 10 to 20 ft). This fault location is generally consistent with tectonic geomorphic lineaments mapped during our desktop analysis and is 92 ft (28 m) east of the Graymer (2000) mapping.

At Field localities 4 and 5, LCI confirmed a steep break in slope associated with the eastern Hayward fault trace and outcrops of rock comprising Jurassic units (i.e., basalt, diabase, graywacke, mélange or Jsv/ Jb – see Photo 2).

To the southwest along the Chabot fault (Field Locality 6), we mapped the Chabot fault based on juxtaposition of bedded sedimentary rocks of the Cretaceous Great Valley units (Kjm) on the east juxtaposed against diabase-basalt and graywacke on the west (Photos1 and 2). The faulted

Photo 1. Field Locality 6 – fault contact between Jurassic and Cretaceous units along Scout Rd.

contact is aligned with a topographic saddle to the northwest and a drainage deflection, and a northwest-trending linear drainage to the southeast. This fault location is 66 ft (20 m) east of the Graymer (2000) strand (Figure 1) but is consistent with geologic map relationships shown by the author.

Field locality 7 is further southeast along Scout Rd. and consists of dipping shale beds of the Cretaceous sedimentary unit (Kjm; Photo 3). This road cut exposure is a near vertical wall located on the north side of Scout Rd. directly northeast of Montera School and the linear drainage that runs along Scout Rd.

Field localities 8, 9,10, and 11 are southwest across Scout Rd. and the linear drainage within Montera school. These localities consist of outcrops of Jurassic serpentinite, mélange, and/ or volcanic rocks (sp, Jsv, Jb from Graymer, 2000) similar to those observed at locality 6 (Photo 2). These units are exposed on the steep canyon wall on the west side of the incised linear drainage channel but could not be observed in the thalweg of the creek or beneath Scout Rd. The fault

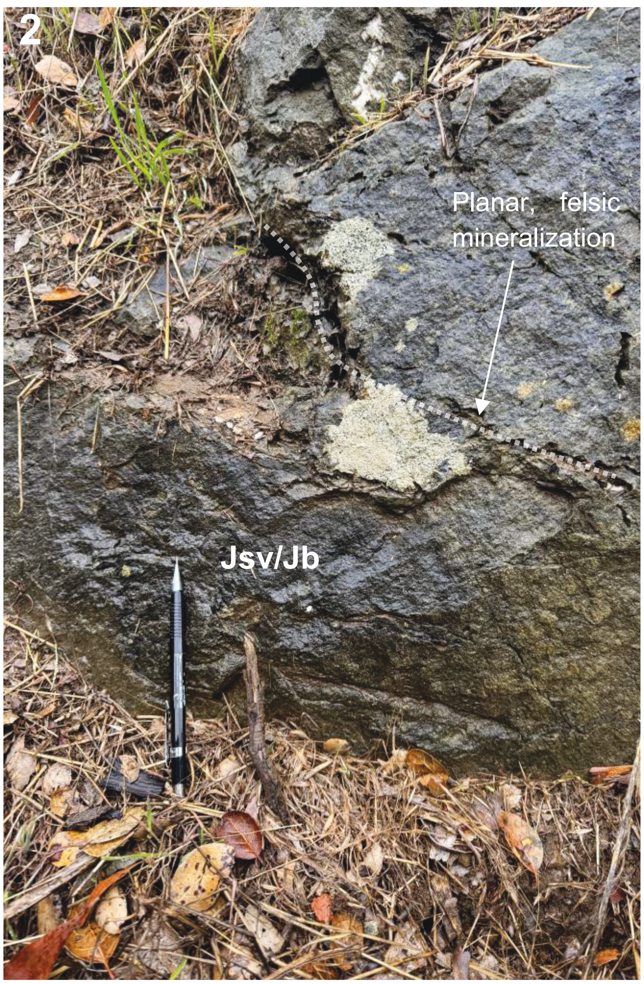

Photo 2: Field Locality 6 – Jurassic diabase/ basalt or graywacke (Jsv/ Jb) with planar, secondary felsic mineralization; Photo 3: Field Locality 7 – dipping beds in the Cretaceous unit (Kjm) directly northeast of linear drainage.

contact separating these units is constrained within the width of the creek drainage (approximately 100 ft) between Cretaceous and Jurassic units are exposed on either side.

2.3 FAULT LOCATION UNCERTAINTY ZONES

Fault location uncertainty can be an important consideration for siting infrastructure within the Moraga-Oakland utility corridor (Figures 1 and 2). The following section summarizes the basis for the fault location uncertainty zones in the area of interest.

2.3.1 Technical approach

LCI developed fault location uncertainty zone widths using a combination of site-specific geomorphic and geologic mapping, field reconnaissance, a review of published literature (Petersen et al., 2011; Chen et al., 2013), and professional judgment. Petersen et al. (2011) and Chen et al. (2013) develop fault zone width uncertainties for Holocene faults based on comparisons between pre-earthquake fault mapping (e.g., CGS FERs) and actual historical ruptures for strike-slip faults in California. Table 1 combines Petersen et al. (2011) uncertainty estimates (see their Tables 2 and 3) to inform fault local uncertainty zone widths. Both Petersen et al. (2011) and Chen et al. (2013) conclude that: (1) the width of the fault location uncertainty zone should expand with decreasing confidence in the fault mapping and an increase in fault zone complexity; and (2) uncertainties can be narrowed when additional data is available (e.g., LiDAR or site-specific trench data) (Petersen et al., 2011). Following this general approach, PG&E incorporates the standard deviation of Petersen et al. (2011) (Table 1) to develop initial fault location uncertainty zones for unstudied or poorly assessed faults. PG&E does not include the standard deviations of Chen et al. (2013) because this paper remains unpublished and is not part of a peer-reviewed journal, and also contains an error within the calculations. Lastly, for the PG&E fault location study, uncertainty zones are not always measured for every mapped fault strand. For example, there is judgement imparted where the zones may be applied to only LCI project-specific mapping and/or combined with fault strands mapped by others.

Using the fault location uncertainties from Petersen et al. (2011), LCI followed a three-step process to develop the fault location uncertainty zones. First, the width of the zone considers a 2-standard deviation buffer on either side of the fault trace (or fault traces) and includes the confidence in the available mapping, as well as fault zone complexity (Table 1). For example, an accurately located fault strand has a standard deviation of 27 m, thus a two-sigma width on either side of the fault results in a 108-m-wide zone (or a 54-meter-wide zone on either side of the fault). A single standard deviation or multiple standard deviations can be used along the length of the fault if mapping confidence changes (e.g., the zone may widen if the fault mapping becomes increasingly uncertain). In the second step, additional information is considered at each crossing to evaluate whether the uncertainty zone widths should be reduced or widened. This site-specific and local fault characterization information increases confidence on the likelihood of identifying all potential fault-related features at the crossings. Third, the uncertainty zones are then reviewed again for lateral continuity or fault terminations.

Table 1. Fault Mapping Uncertainties (Petersen et al., 2011)

MAPPING ACCURACY	*STANDARD DEVIATION ON FAULT (M)	COMPLEXITY	*STANDARD DEVIATION ON FAULT (M)
All	**53**	Simple, concealed	**62**
Accurate	**27**	Simple, inferred	**50**
Approximate	**44**	Complex, concealed	**116**
Concealed	**66**	Complex, inferred	**116**
Inferred	**73**		

**Values listed above include the two-sided standard deviations (rounded to the nearest whole number) from Petersen et al. (2011)'s tables 2 and 3, which are the recommended uncertainty terms to use as part of the fault zone construction. These values represent standard deviation values in meters away from the mapped fault trace.*

2.3.2 Hayward-Chabot Fault Uncertainty Zones

Based on the information summarized above, LCI developed fault location uncertainty zones for fault strands that intersect the Moraga-Oakland utility corridor east of Highway 13, including two traces of the Hayward fault and a strand of the Chabot fault (Figure 2).

The Hayward fault strands are moderately well-constrained based on creep features and tectonic geomorphology and consistently mapped by various authors (Herd, 1978; Graymer, 2000; Lienkaemper, 2008; Figure 2). Along Scout Road (field locality 4; Figure 2), a steep break in slope observed directly west of the road confirms the approximate easternmost location of the Hayward fault through the corridor. This zone is east of the main creeping strand mapped by Lienkaemper (2008) and is considered an easternmost limit of the uncertainty zone. This trace is in the vicinity of a slight left bend in the fault (PG&E V15, 2022) that may result in a broader deformation pattern along this section of the fault. Several tectonic geomorphic features such as scarps, troughs, and deflected/ linear drainages correlate the creep observation sites by Lienkaemper (2008). Thus, the location of the Hayward fault is confirmed based on creep observations (Lienkaemper, 2008), geomorphic mapping, and observations made during field reconnaissance.

On the basis of these findings, LCI developed an approximately 279 to 335-ft-wide (85 to 102-m-wide) wide fault location uncertainty zone that parallels the western creeping strand and the eastern strand (PG&E, 2022) of the Hayward fault encompassing the western portion of the Moraga-Oakland utility corridor (Figure 2). This zone was developed based on a starting fault buffer ~289-ft-wide (88-m-wide) because the more prominent, western strand is approximately located (i.e., one standard deviation is ~44-m-wide; Table 1). This initial width was reduced so that the easternmost limit of the zone generally coincides with the break in slope observed at field locality 4. This topographic feature represents the eastern limit of the break in slope associated with the eastern Hayward fault strand (Figure 2). East of this break in slope bedrock forms broadly sloping surfaces that appear unfaulted and provide a reasonable maximum limit for the fault location uncertainty zone.

As discussed above, LCI mapped the Chabot fault based on juxtaposition of bedrock units and alignment of erosional geomorphic features (Figure 2). The geomorphology along the fault is relatively poorly expressed with limited evidence of significant late Pleistocene and Holocene faulting and LCI concurs with past assessments by (Herd 1978; WLA, 1996) that the Chabot fault is not a Holocene fault.

To assist with the utility alignment, LCI developed a 289-ft-wide (88-m-wide) wide fault location uncertainty zone that parallels the revised Chabot fault trace study (Figure 2). This zone was developed based on a starting fault buffer 545-ft-wide (166-m-wide) because the here is mapped as strands approximately located (i.e., one standard deviation is ~44-m-wide; Table 1). This initial width was reduced was reduced to a buffer width ~88-ft-wide (44-m-wide) for a total width of 289-ft-wide (88-m-wide) based on surface constraints from combination of the geomorphology along the fault and exposures along road cuts (Field Locality 6; Figure 1). The fault zone is also tapered based on our judgment where the fault is constrained through surface mapping (Field locality 3).

3.0 SUMMARY AND CLOSING

In summary, LCI evaluated the location of potential Hayward fault and Chabot fault strands within the Moraga-Oakland utility corridor north of Highway 13 in Oakland, California (Figures 1 and 2). Our results indicate the presence of possible Holocene Hayward fault strands along the southwestern margin of the Moraga-Oakland utility corridor. LCI also evaluated and re-mapped the Chabot fault through the northeastern part of the utility corridor. All available studies indicate the Chabot fault is inactive (Pre-Holocene; Herd, 1978; WLA, 1996) and LCI agrees with this assessment based on our review of geomorphology and local fault studies. To assist with locating PG&E infrastructure within the corridor, LCI developed two fault location uncertainty zones using uncertainty estimates from the peer reviewed literature, site information, and our professional judgement.

LCI appreciates the opportunity to assist PG&E Geosciences on this interesting fault location study.

Please contact us if you have any questions.

Sincerely,

LETTIS CONSULTANTS INTERNATIONAL, INC.

CERTIFIED ENGINEERING GEOLOGIST
ROBERT W. GIVLER
Exp. 9/30/24
NO. 2533
STATE OF CALIFORNIA

Ian McGregor
Senior Staff Geologist
mcgregor@lettisci.com

Robert Givler, C.E.G
Principal Geologist
givler@lettisci.com

4.0 REFERENCES CITED

Case, J.E., 1968, Upper Cretaceous and Lower Tertiary Rocks, Berkeley and San Leandro Hills, California: Contributions to General Geology, Geological Survey Bulletin 1251-J.

Chen, R., Dawson, T.E., and Wills, C.J., 2013, Quantifying Surface Fault Rupture Location Uncertainty for Lifeline Crossings: U.S. Geological Survey Final Technical Report, National Earthquake Hazards Reduction Program Award Number G11AP20040, 51p. available at https://earthquake.usgs.gov/cfusion/external_grants/reports/G11AP20040.pdf.

d'Alessio, M. A., I. A. Johanson, R. Bürgmann, D. A. Schmidt, and M. H. Murray, 2005, Slicing up the San Francisco Bay Area: Block kinematics and fault slip rates from GPS-derived surface velocities, J. Geophys. Res. Solid Earth 110, B06403, doi 10.1029/2004JB003496.

Dawson, T.E., and Weldon, R.J., 2013, Appendix B: Geologic slip-rate data and geologic deformation model: U.S. Geological Survey Open-File Report 2013-1165-B, and California Geological Survey Special Report 228-B

ESA Consultants Inc./ William Lettis & Associates, Inc., 1996, Seismic Evaluation of South Reservoir Embankments: unpublished consulting report for East Bay Municipal Utility District dated December, 1996.

Evans, E.L., Loveless, J.P., and Meade, B.J., 2012, Geodetic constraints on San Francisco Bay Area fault slip rates and potential seismogenic asperities on the partially creeping Hayward fault, Journal of Geophysical Research, 117, B03410, doi:10.1029/2011JB008398.

Field, E.H., Biasi, G.P., Bird, P., Dawson, T.E., Felzer, K.R., Jackson, D.D., Johnson, K.M., Jordan T.H., Madden, C., Michael, A.J., Milner, K.R., Page, M.T., Parsons, T., Powers, P.M., Shaw, B.E., Thatcher, W.R., Weldon, R.J., Seng, Y., 2015, Long-term time-dependent probabilities for the Third Uniform California Earthquake Rupture Forecast (UCERF3), Bulletin of the Seismological Society of America, v. 105, no. 2a, p. 511–543.

Field, E.H., Biasi, G.P., Bird, P., Dawson, T.E., Felzer, K.R., Jackson, D.D., Johnson, K.M., Jordan, T.H., Madden, C., Michael, A.J., Milner, K.R., Page, M.T., Parsons, T., Powers, P.M., Shaw, B.E., Thatcher, W.R., Weldon, R.J., II, and Zengand, Y., 2013, Uniform California Earthquake Rupture Forecast, Version 3 (UCERF3)—The Time-Independent Model: U.S. Geological Survey Open-File Report 2013-1165.

Graymer, R.W., 2000, Geologic map and map database of the Oakland Metropolitan area, Alameda, Contra Costa, and San Francisco Counties, California; U.S. Geological Survey Miscellaneous Field Studies Report 2342, http://pubs.usgs.gov/mf/2000/2342/

Graymer, R. W., B. C. Moring, G. J. Saucedo, C. M. Wentworth, E. E. Brabb, and K. L. Knudsen (2006). Geological map of the San Francisco Bay region, U.S. Geol. Survey Scientific Investigation Map 2918, scale 1:250,000.

Herd, D.G., 1978, Map of Quaternary faulting along the Hayward fault zone: U.S. Geological Survey Open-File Report 78-308.

InfraTerra, 2021, Fault Creep Review across PG&E Gas Transmission System in San Francisco Bay Area: 5-year progress report for Marker Ball Array Surveys, unpublished consulting report, dated June 29, 2021.

JCP-Engineers & Geologists, Inc., 1980, Engineering Geologic Study Proposed Office Building off of Antioch Street Oakland, California: Unpublished consulting report filed with the City of Oakland (AP#1253)

Johnson, K. M., J. R. Murray, and C. Wespestad, 2022, Creep Rate Models for the 2023 US National Seismic Hazard Model: Physically Constrained Inversions for the Distribution of Creep on California Faults, Seismol. Res. Lett. V. 9, no. 6, 3151-3169, doi: 10.1785/0220220186.

Lettis, W.R., 2001, Late Holocene Behavior and Seismogenic Potential Of The Hayward-Rodgers Creek Fault System In The San Francisco Bay Area, California: in H. Ferriz (ed.), Engineering Geology Practice in Northern California, Association of Engineering Geologists, Special Publication 12, Bulletin 210, p. 167-177.

Lienkaemper, J.J. 1992. Map of recently active traces of the Hayward Fault, Alameda and Contra Costa counties, California

Lienkaemper, J.J. 2008. Digital database of recently active traces of the Hayward Fault, California. Original 2006, revised 2008. US Geological Survey Data. Series 177, v.1.1. Available at http://pubs.usgs.gov/ds/2006/177/.

Lienkaemper, J.J., Baker, B. and McFarland, F.S., 2006. Surface slip associated with the 2004 Parkfield, California, earthquake measured on alinement arrays. Bulletin of the Seismological Society of America, 96(4B), pp.S239-S249.

Lienkaemper, J.J., McFarland, F.S., Simpson, R.W., and Caskey, S.J., 2014, Using surface creep rate to infer fraction locked for sections of the San Andreas fault system in northern California from alignment array and GPS data: Bull. Seism. Soc. Am., v. 104, no. 6, 21 p; doi: 10.1785/0120140117.

Lienkaemper, J.J., and Borchardt, G., 1996, Holocene slip rate of the Hayward fault at Union City, California: Journal of Geophysical Research, v.101, no. B3, p. 6099-6108.

McFarland, F.S., Lienkaemper, J.J., Caskey, S.J., and Elliot, A.J., 2017, Data from Theodolite Measurements of Creep Rates on San Francisco Bay Region Faults, California (ver. 2.1, October 2022): U.S. Geological Survey data release, https://doi.org/10.5066/F76W9896.

Kaldveer, P. and Associates, 1985, Geotechnical Engineering Services for Proposed Retail Building, Oakland, California: Unpublished consulting report filed with the City of Oakland (AP#1886)

Kaldveer, P. and Associates, 1988, Fault Rupture Hazard Investigation for Montclair East Additions Oakland, California: Unpublished consulting report filed with the City of Oakland (AP#2210)

Petersen, M.D., Dawson, T.E., Chen, R., Cao, T., Wills, C.J., Schwartz, D.P., and Frankel, A.D., 2011, Fault displacement hazard for strike-slip faults: Bulletin of the Seismological Society of America, 101(2), pp. 805-825.

Pacific Gas and Electric Company (PG&E), 2022, Fault database, version 15 titled "Geosciences_FAULTS_V15.gdb", developed by InfraTerra Inc.

Pacific Gas and Electric Company (PG&E), 2024, Utility locations, kmz titled "Oakland_Power_Reinforcement_Project_SNct"

Ponce, D.A., Hildenbrand, T.G., and Jachens, R.C., 2003, Gravity and magnetic expression of the San Leandro gabbro with implications for the geometry and evolution of the Hayward Fault Zone, northern California: Bulletin of the Seismological Society of America, v. 93, p. 14–26

Purcell, Rhoads, & Associates, 1985, Fault Evaluation Study - Corner of Antioch Street Montclair, California Site Located at and Mountain Northwest Boulevard, Unpublished consulting report filed with the City of Oakland (AP#1863)

Radbruch-Hall, D.H., 1974, Map Showing Recently Active Breaks along the Hayward Fault Zone and the Southern Part of the Calaveras Fault Zone, California: U.S. Geological Survey Misc. Investigations Series Map I-813, scale 1:24,000

Radbruch, D.H., 1969, Areal and engineering geology of the Oakland East quadrangle, California: U.S. Geological Survey Map GQ-769, 1:24,000 scale

Schwartz, D.P., Lienkaemper, J.J., Hecker, S., Kelson, K.I., Fumal, T.E., Baldwin, J.N., Seitz, G.G., Niemi, T.M., 2014, The earthquake cycle in the San Francisco Bay region: A.D. 1600-2012: Bulletin of the Seismological Society of America, v., 104, no. 3, p. 1-30.

Smith, T.C., 1980, Fault Evaluation Report FER-102, California Division of Mines and Geology, December 15, 1980

U.C. Santa Barbara (UCSB) Library, 2024, UCSB Library Aerial Photography FrameFinder Online Tool, Available online at the following link: http://mil.library.ucsb.edu/ap_indexes/FrameFinder/, last accessed [1/2/2024]

USGS, 2021, USGS CA AlamedaCo2 2021 LiDAR data collected in 20182019-2021, available on-line at: https://portal.opentopography.org/usgsDataset?dsid=CA_AlamedaCo_2_2021

Western Geologic Consultants, 1976, Evaluation of potential for surface faulting, Montclair parking structure, Oakland, California: Unpublished consulting report filed with the City of Oakland (AP#370)

Working Group on California Earthquake Probabilities (WGCEP), 2003. Earthquake probabilities in the San Francisco Bay region: 2002-2031: US Geological Survey Open-File Report 03-214.

Working Group on California Earthquake Probabilities (WGCEP), 2008, The Uniform California Earthquake Rupture Forecast, Version 2 (UCERF2), USGS Open-file report 2007-1437 and CGS Special Report #203 V. 10

Williams, P., 2011, Rate constraints for the Northern Hayward Fault at Berkeley: evaluation of the 335-meter Strawberry Creek offset, Final Technical Report for U.S. Geological Survey NEHRP Award G09AP00006. 14 p

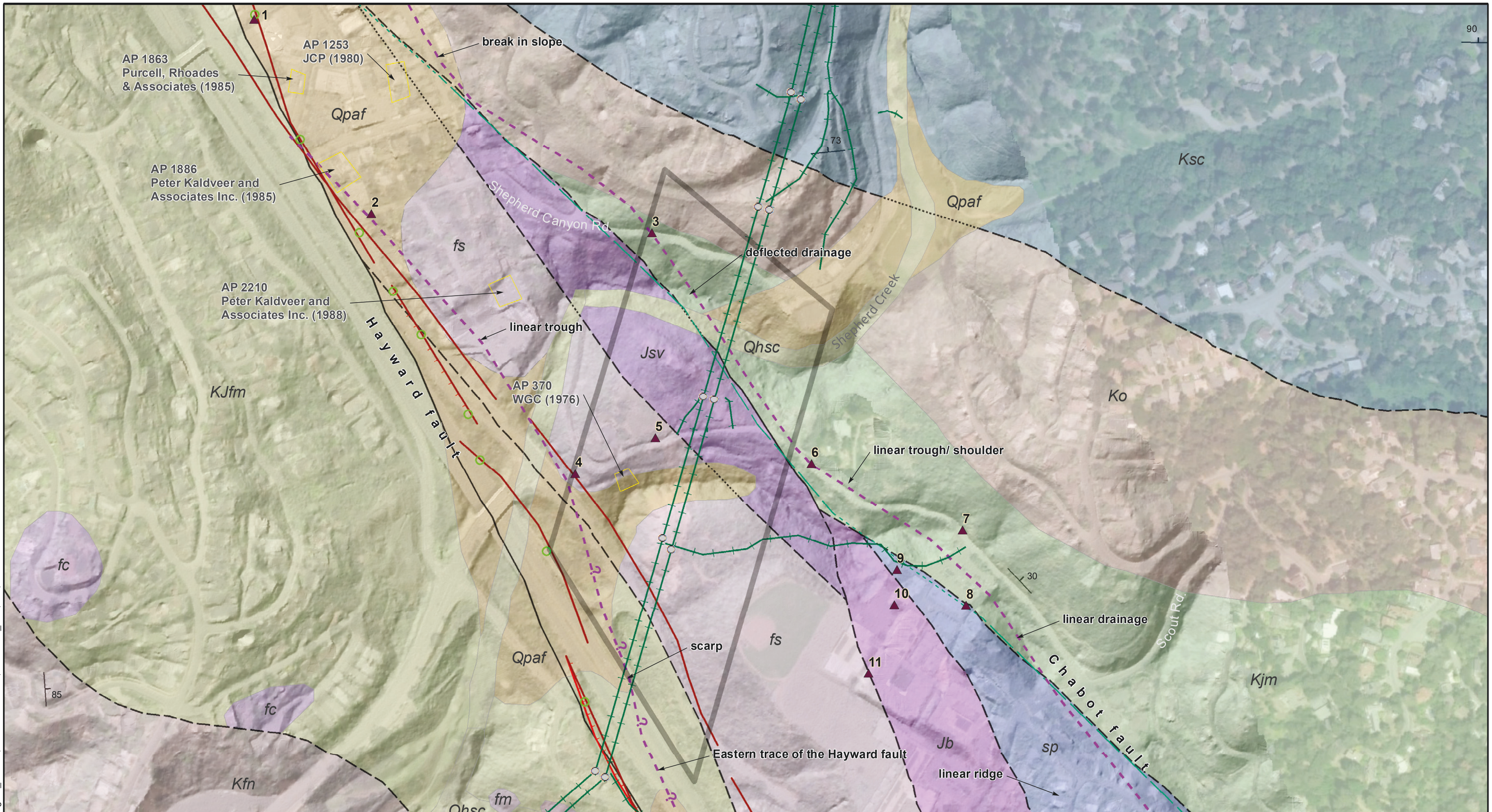

EXPLANATION

PG&E tower location (existing)

PG&E powerline (exisitng)

Area of Interest

Fault (PG&E 2022, v15) solid where certain, dashed where inferred

Historic Fault (PG&E 2022, v15) solid where certain, dashed where inferred

LCI (this study)

Revised fault location, solid where certain, dashed where inferred

Field locality

Lienkaemper (2008)

Fault, solid where certain, dashed where inferred

Creep location

Regular alinement array

Note:
Map rotation: 50°

0 100 200 ft
0 25 50 m

Map projection and scale:
NAD 1983 UTM Zone 10N, 1:4,000

NOTE: Geologic mapping from Graymer (2000); see text for explanation of geologic units

Hayward-Chabot Utility Corridor
Geologic Data and
Revised Fault Mapping

PG&E 2024 FAULT LOCATION STUDY

Lettis Consultants International, Inc. | Figure **1**

File path: S:\1005_121\00_Figures\Figure_01.mxd; Date: 01/26/2024; User: smt_user, LCI; Rev.1

Preliminary and Subject to Change Based on CPUC Requirements, Final Engineering, and Other Factors

EXPLANATION

PG&E tower location (existing)

PG&E powerline (exisitng)

Area of Interest

Fault (PG&E 2022, v15) solid where certain, dashed where inferred

Historic Fault (PG&E 2022, v15) solid where certain, dashed where inferred

LCI (this study)

Revised fault location, solid where certain, dashed where inferred

Field locality

Fault location uncertainty zone

Lienkaemper (2008)

Fault, solid where certain, dashed where inferred

Creep location

Regular alinement array

Note:
Map rotation: 50°

0 100 200 ft
0 25 50 m

Map projection and scale:
NAD 1983 UTM Zone 10N, 1:4,000

Hayward-Chabot Utility Corridor
Fault Uncertainty Zones

PG&E 2024 FAULT LOCATION STUDY

Lettis Consultants International, Inc. | Figure 2

File path: S:\1005_121\00_Figures\Figure_02_v2.mxd; Date: 01/26/2024; User: smt_user, LCI; Rev.1

Preliminary and Subject to Change Based on CPUC Requirements, Final Engineering, and Other Factors